

tial condition can be satisfied using Control (IC) illustrated for this application. Although a proportional approach is applied in [6] the tracking control is only valid when the reference signal is periodic. This is not the case in general for a real-time application: causing an opening process depends on the desired signal and the magnetic field control. The IC, using the position of the previous iteration to modify the input of the next iteration in order to improve the tracking of a given trajectory. By choosing a sufficiently small trajectory, a better tracking is possible, so should the impact locality.

The model and control difficulties are summarized in Section 2. Section presents an analysis of IC theory. Modeling due to inductance is presented in Section 4. Experimental results are found in Section 5.

2 Model and control Difficulties

2.1 System model

Nonlinear system model is developed in [7] and later extended to include impact dynamics in [5]. The model consists of four states: the actuator distance from the catching coil, z , the actuator velocity, v , the current in the lower coil, i_l , and the current in the upper coil, i_u . To achieve fast localization a pulse-width modulation (PWM) technique is developed in [7] to define the holding current to z of trajectory. Thus the holding current has little influence on the motion of the actuator. By assuming that fall opening and closing are identical, the four state system is defined as follows: the state system

i_l Catching coil current [A]
 z Distance from the catching coil [m]
 v Actuator velocity [m/s]

The tracking equation of motion is

$$\frac{di_l}{dt} = \frac{V_c - r i_l + \chi_1(i_l, z) v}{\chi_2(z)} \quad (1)$$

$$\frac{dz}{dt} = 1000v \quad (2)$$

$$\frac{dv}{dt} = \frac{1}{m} (-F_{mag}(i_l, z) + k_s(4 - z) - bv) \quad (3)$$

where

$$\chi_1(i_l, z) = \frac{2k_a i_l}{(k_b + z)^2} \quad (4)$$

$$\chi_2(z) = \frac{2k_a}{1000(k_b + z)} \quad (5)$$

$$F_{mag}(i_l, z) = \frac{k_a i_l^2}{(k_b + z)^2} \quad (6)$$

written compactly as

$$\frac{dx}{dt} = f(x, V_c) \quad (7)$$

$$x = [i_l \ z \ v]^T \quad (8)$$

$$y = [0 \ 1 \ 0] x \quad (9)$$

where V_c is the catching coil voltage [V], i_l is the current in the lower coil [A], k_s is the spring stiffness [N/m], b is the damping [Ns/m], F_{mag} is the magnetic force due to the catching coil [N], $\chi_1 v$ is the actuator EMF [V], and χ_2 is the inductance [H], and y is the output.

2.2 Control difficulties

The main difficulty comes from a lack of control authority of the actuator motion away from the catching coil and the current in the catching coil. A large distance from the catching coil the magnetic force is much smaller than the spring force, as shown in figure 2. Therefore the system is dominated by the spring force and the control has no authority of the actuator motion at a large distance from the catching coil. The magnetic force does have influence on the actuator motion, but manipulation of equation (1) fails that the input voltage has little influence on the current dynamics. To demonstrate this consider the current dynamics

$$\frac{di_l}{dt} = 1000 \left(\frac{(V_c - r i_l)(k_b + z)}{2k_a} + \frac{i_l v}{(k_b + z)} \right). \quad (10)$$

Not that $k_b \ll 1$ and z is approaching zero. Then placing the term $k_b + z$ with the denominator $\varepsilon = k_b + z$, we get

$$\frac{di_l}{dt} = 1000 \left(\frac{(V_c - r i_l)\varepsilon}{2k_a} + \frac{i_l v}{\varepsilon} \right). \quad (11)$$

The following are the catching coil input, V_c has little effect on the current dynamics. Physically, this is caused by the actuator EMF and the changing inductance.

To summarize, a good design for a tracking controller should

- Initially adjust the current in the input can influence the current dynamics in preparation for when the actuator is near the catching coil.
- Apply high frequency at the end of the trajectory to counteract the changing actuator EMF and inductance.

In [4, 5] this is accomplished through the use of linear and nonlinear control respectively.

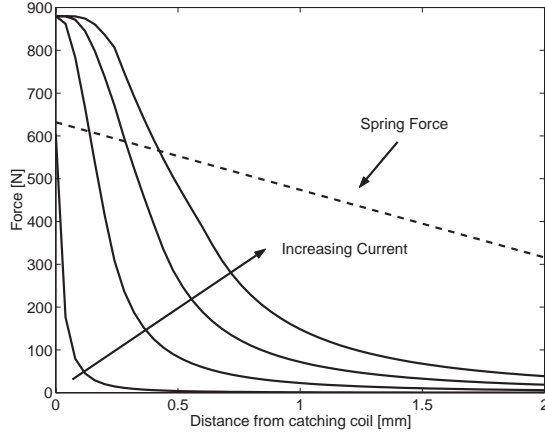


Figure 2: Magnetic force vs. position for different current values.

Linear feedback control analysis and design is presented in [4]. Vt o tag R f d: ac7 cont oll id ign d and im pl m t d to account fo th changing cont ol author ity. Th g t tag of th f d: ac7 (hich act fo d i tanc g at than m m a y f om th catching coil) p naliz Ccu nt much m than position o f locity in th R optimization. V th f d: ac7 ha cont ol author ity of cu nt du - ing th i m i t i c a l to a i th cu nt to C m n o i m a l catching falu , h il adju t i n g h i g h t y f o d f i a t i o n i n p o s i t i o n and f locity. a th catching coil (d i tanc l C than m m a y) th cont oll C i t h C o t h C o n d t a g . In th C o n d t a g th f d: ac7 p naliz C p o s i t i o n and f locity h a f i l y i n th R optimization, to n e w that th a m t u i C o u g h t i n t o c o n t a c t i t h th catching coil. C u n t i C n o t p naliz d i n th C o n d t a g a t : c o m C i n g u l a p t u : d n a th catc hing coil, quation (), and ha C n m f d f i a m d l d u c t i o n [4]. Th i C o n t o l l a c h i f C i m p a c t f l o c i t y C i t h a m a n o f . 6 m C

The linear control law for V_c is a static feedback control authority: v is proportional to the dc average current distance (condition tag). It is a gain to stabilize the system and the load to frequency actuator saturation at the catching coil. V_m is an appropriate solution to the nonlinear feedback law

$$V_c = \frac{K_1}{\gamma + z} v + \frac{K_2}{\beta + z} \quad (2)$$

design in [5]. Since K_1 , K_2 , γ , and β are adjustable gains. The input V_c is proportional to the dc average distance: v is a differentiating effect of the ac7 EM and changing inductance at the catching coil. V_m is a feedback from the catching coil with input offset gain sufficient to adjust current in preparation for catching the actuator. The feedback law achieves impact force with a man of . 6 m C

In [4, 5] an addy current control is used to manage the a -

ntu d i tanc , and a nonlinear o: C f i C h m t d to t i a t th u n m a d t a t C a n d g l t th n o i s y p o s i t i o n m a u m t . Th n o n l i n a o: C f i C i f n : y

$$\frac{d\hat{x}}{dt} = f(\hat{x}, V_c) + L(y - \hat{y}) \quad (3)$$

h \hat{x} i th t i a t d t a t f c t o [\hat{i} \hat{z} \hat{v}] ^T , th gain m i x i C h o n : y u i n g a a l a n g l t , y i C th m a u d p o s i t i o n , \hat{y} i th t i a t d p o s i t i o n , and th function $f(\hat{x}, V_c)$ i th C a m a C q u a t i o n (7).

To improve the transient response of the closed-loop system from cycle to cycle using an iterative learning control algorithm [6]. Manufacturing variation, disturbance, and a non-zero initial condition are not easily achieved during the transient response of the system with a feedback loop. The feedback function is a path in the parameter space (i. .5 time constant, hence the gain is increasing at the path: \hat{z} in [6] is a gain, \hat{v} with an I C. Using the technique of the previous paper, the function $f(\hat{x}, V_c)$ is the input of the next iteration to decrease the transient response. Implementation is associated with applying an I C to the EMV actuator a in- f i g a t d , and x p i m m t a l u t a p C a t d .

3 Iterative Learning Controller

3.1 ILC by singular value decomposition

An iterative learning controller exploits the repetitive nature of a system to improve the tracking of a desired trajectory, y_d , from cycle to cycle.

The input and the output of the system are $u[k]$ and $y[k]$. Since $u[k]$ and $y[k]$ are the k^{th} input and output trajectory respectively. The system is a mapping $\Gamma: R^n \rightarrow R^n$ as $y[k] = \Gamma(u[k])$. Using the implicit function theorem $\{h[n]\}$ of the closed loop discrete linearized system into the convolution matrix

$$P = \begin{bmatrix} h[1] & 0 & 0 & \dots & 0 \\ h[2] & h[1] & 0 & \dots & 0 \\ \vdots & \vdots & \ddots & \ddots & \vdots \\ h[N-1] & h[N-2] & \dots & h[1] & 0 \\ h[N] & h[N-1] & \dots & h[2] & h[1] \end{bmatrix} \quad (4)$$

that provides a linear approximation of the system at the equilibrium $\Gamma(u[k]) \cong Pu[k]$.

The purpose of the ILC is to find the input, u^* , such that $y_d \cong Pu^*$. A linear ILC algorithm is

$$u[k+1] = Su[k] + E(y_d - y[k]) \quad (5)$$

the matrix S is the right on the previous input and the matrix E is the right on the previous output. S and E are defined to be constant such that

$$u^* = \lim_{k \rightarrow \infty} u[k]. \quad (6)$$

By using condition (5), let S and E be given by

$$S = I, \text{ and } E = \frac{1}{\sigma_o} RL^T \quad (7)$$

where R and L contain the right and left singular vectors of the singular value decomposition, $P = L\Lambda R^T$. Λ is a diagonal matrix whose elements are the singular values of the convolution matrix, σ_i , arranged in descending order, $\sigma_o \geq \sigma_1 \geq \dots \geq \sigma_i \geq \dots \geq \sigma_{N-2} \geq \sigma_{N-1}$.

By using $y[k] \cong Pu[k]$, equation (5) is written as

$$u[k+1] = Su[k] + E(y_d - Pu[k]) \quad (8)$$

$$\Rightarrow R^T u[k+1] = \left(I - \frac{1}{\sigma_o} \Lambda \right) R^T u[k] + \frac{1}{\sigma_o} L^T y_d \quad (9)$$

By applying the linear transformation $v[k] = R^T u[k]$, and $\mu = L^T y_d$ we obtain

$$v[k+1] = \left(I - \frac{1}{\sigma_o} \Lambda \right) v[k] + \frac{1}{\sigma_o} \mu \quad (10)$$

which can be written into compact notation as

$$v_i[k+1] = \left(1 - \frac{\sigma_i}{\sigma_o} \right) v_i[k] + \frac{1}{\sigma_o} \mu_i \quad \forall i \in [0, N-1]. \quad (11)$$

The choice of S and E yields a decoupled learning algorithm. The convergence of the ILC is guaranteed by the stability of the N scalar equations in (11). Each eigenvalue is given by $\lambda_i = \left(1 - \frac{\sigma_i}{\sigma_o} \right)$. Convergence is guaranteed for each scalar equation if $|\lambda_i| < 1$. For $\sigma_o \geq \sigma_i > 0$, $|\lambda_i| < 1$ is satisfied. Solving equation (11) yields

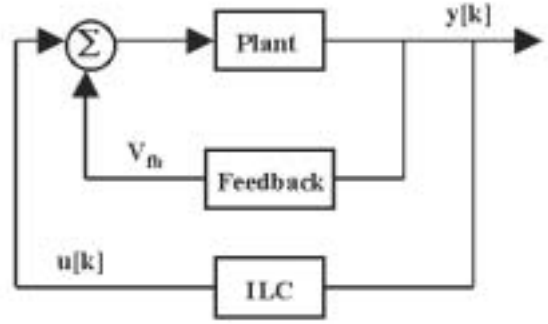
$$v_i[k] = \left(1 - \frac{\sigma_i}{\sigma_o} \right)^k v_i[0] + \frac{1 - \left(1 - \frac{\sigma_i}{\sigma_o} \right)^k}{\sigma_i} \mu_i \quad (12)$$

which converges to

$$\lim_{k \rightarrow \infty} v_i[k] = v_i^* = \frac{1}{\sigma_i} \mu_i. \quad (13)$$

Since the convergence rate is determined by $1 - \frac{\sigma_i}{\sigma_o}$ and v_i^* is proportional to σ_i^{-1} , output components that require a larger input than output components requiring a larger input, which is crucial in helping to a field actuator saturation.

Then using equation (12): we substitute into y_d and u and



the iterative learning control is applied to the EMV actuator

$$R^T u^* = \Lambda^{-1} L^T y_d$$

which after noting that $R^T = R^{-1}$ and $L^T = L^{-1}$ yields

$$u^* = R\Lambda^{-1} L^T y_d. \quad (14)$$

For convergence the plant output is equal to the desired output

$$\begin{aligned} y &= Pu^* \\ \Rightarrow y &= L\Lambda R^T u^* \\ \Rightarrow y &= L\Lambda R^T R\Lambda^{-1} L^T y_d \\ \Rightarrow y &= y_d. \end{aligned}$$

So in consequence the iterative learning control is ending the plant information cycle to cycle to achieve tracking of the desired output.

3.2 ILC as applied to the EMV actuator

In this paper, the ILC is applied to the EMV actuator as shown in figure 1. Since the output, y , is a distance from the catching coil, and the input, u , is a pulse for a deflag.

To properly define the linear and nonlinear system (7), let

$$V_c = V_{fb} + V_{ff} \quad (15)$$

where V_{fb} is the feedback voltage from the nonlinear controller (2), and V_{ff} is the feedforward voltage, u , from the ILC explained in section 3.1. Substituting into equation (7), the closed-loop continuous dynamic

$$\frac{di_{cl}}{dt} = \frac{V_{fb} + V_{ff} - ri + \chi_1 v}{\chi_2} \quad (26)$$

$$\frac{di_{cl}}{dt} = \frac{\frac{K_1}{\gamma+z} v + \frac{K_2}{\beta+z} + V_{ff} - ri + \chi_1 v}{\chi_2} \quad (27)$$

The A_{cl} and B_{cl} matrix of the closed loop linear system

$$\frac{dx}{dt} = A_{cl}x + B_{cl}V_{ff} \quad (28)$$

$$y = [0 \ 1 \ 0] x \quad (29)$$

analytically

$$A_{cl} = \begin{bmatrix} \frac{\partial}{\partial i} \left(\frac{di_{cl}}{dt} \right) \Big|_{x=x_{eq}} & \frac{\partial}{\partial z} \left(\frac{di_{cl}}{dt} \right) \Big|_{x=x_{eq}} & \frac{\partial}{\partial v} \left(\frac{di_{cl}}{dt} \right) \Big|_{x=x_{eq}} \\ 0 & 0 & \frac{\partial}{\partial v} \left(\frac{dz}{dt} \right) \Big|_{x=x_{eq}} \\ \frac{\partial}{\partial i} \left(\frac{dv}{dt} \right) \Big|_{x=x_{eq}} & \frac{\partial}{\partial z} \left(\frac{dv}{dt} \right) \Big|_{x=x_{eq}} & \frac{\partial}{\partial v} \left(\frac{dv}{dt} \right) \Big|_{x=x_{eq}} \end{bmatrix} \quad (30)$$

and

$$B_{cl} = \begin{bmatrix} \frac{\partial}{\partial V_{ff}} \left(\frac{di}{dt} \right) \Big|_{x=x_{eq}} \\ 0 \\ 0 \end{bmatrix} \quad (31)$$

where $x_{eq} = [i_e \ 0 \ 0]^T$ is the equilibrium point, and i_e is the value of current such that $F_{mag}(i_e, 0) = 4k_s$.

The following input-output model is derived from the first-order model and the discrete-time model shown in Fig. 1. The convolution matrix P for the I/O model is the impulse response of the discrete-time system (with a sampling rate of 272 Hz) of equations (28), (29), (30), and (31).

4 Implementation issues

This section presents a methodology to the I/O model to compute nonlinearities, noise, and computational load.

4.1 Computational limitations

The iterative learning control needs to be implemented in an environment (continuous or discrete-time) with computational load constraints: you need to know the computational load in this section to know the computational load can be reduced by careful selection of the parameters: joint and actuator authority.

The main purpose of the I/O model is to achieve the landing of the antenna against the catching coil. Such, it only needs to achieve the tracking of the desired position at the final end of the antenna transition. The partition the output y_c , $y[k] = Pu[k]$, into

$$\begin{bmatrix} y_1 \\ y_2 \end{bmatrix} = \begin{bmatrix} P_1 \\ P_2 \end{bmatrix} u \quad (32)$$

where y_1 and y_2 are the initial and final position of the position trajectory output respectively. The distinction: the initial position is defined by the distance that corresponds to magnetic force higher than the spring force. The magnetic force constant is longer than the equilibrium (load) current value for distance l than l_0 . The output partition is defined as

- y_1 : the position of the position trajectory output for distance l greater than l_0 away from the catching coil
- y_2 : the position of the position trajectory output for distance l less than l_0 away from the catching coil

The following tracking of only y_2 the output in the model is the I/O model reduced to $y_2 = P_2 u$. The computational load is further reduced by taking into account the control authority is calculated in Section 2.2.

The input $y_2 = P_2 u$ can now be calculated as

$$y_2 = [P_{21} \ P_{22} \ P_{23}] \begin{bmatrix} u_1 \\ u_2 \\ u_3 \end{bmatrix} \quad (33)$$

where u_1 contains the input signal applied to the antenna at distance 5 mm away from the catching coil, u_2 contains the input signal applied to the antenna at distance 5 mm and 5 mm away from the catching coil, and u_3 contains the input signal applied to the antenna at distance l less than l_0 away from the catching coil. Similarly, P_{21} is the effect of input applied to the antenna at distance 5 mm away from the catching coil to y_2 , P_{22} is the effect of input applied to the antenna at distance 5 mm and 5 mm away from the catching coil to y_2 , and P_{23} is the effect of input applied to the antenna at distance l less than l_0 away from the catching coil.

The significance of the region on the input u_c can be defined as follows: since the input has little effect on the current dynamics for all distance l , equation (33), the region for the iterative learning control to modify the input force at all distance l from the catching coil, $y < 0.3 \text{ mm}$. Second, at the magnetic force is much less than the spring force at large distance l , the initial force on the iterative learning control should modify the input force when the antenna is far away from the catching coil, $y > 3.5 \text{ mm}$.

The union of the two regions, the iterative learning control only adjusts the first-order model: $l_0 = 5 \text{ mm}$ and

may further catch coil. Vt a catching at of 2
 72 z thi co cond to appo xintly hich i
 th axim uniz that ou poc g: oad cap im m t
 in altim To 7 pth at ic qua , th iz of y_2 i
 to:

The g nal apping mo y d: y th I C i Ch $y_2 = P_{22}u_2$.
 Th ighting at ic C S and E of equation (5) a d t -
 im d: y th ingula falu d comp ition of P_{22} .

Due to apping and ma C m t noi C it i C not po C l to
 haf u_2 ta t and nd xactly at . 5 mand . m a ay
 f om th catch ing coil o i C t po C l to haf y_2 ta t x-
 exactly at . m a y f om th catch ing coil To cla ify, th
 th computation C int oduc additional notation: a d on
 th di C t and f nt C t u ind x th k^{th} it ation of
 th input f oltag , u_2 , hich ha C ngth a C

$$u_2[k][j_u] \text{ fo } j_u \in (0, 30), \quad (4)$$

and d g n $u_2[k][0] = 0$. o di C an C g at than . 5 m
 a ay f om th catch ing coil j_u i C h ld at z o. Vft th
 cont oll d t ct C a position l C than . 5 m a y f om th
 catching coil, j_u inc a C inc m tally ith th C apping
 at .

Simla y , l t u C nd x th k^{th} it ation of th output, y_2 ,
 hich ha C ngth a C

$$y_2[k][j_y] \text{ fo } j_y \in (1, 30) \quad (5)$$

h $y_2[k][j_y]$ C C th ma C d output at th cu nt
 tim C p o di C an C g at than . m a ay f om
 th catching coil j_y i C h ld at . Th C th cont oll 7 p
 iting th falu of $y_2[k][1]$ at ach tim C p Vft th
 cont oll d t ct C a position l C than . m a y f om th
 catching coil, j_y inc a C inc m tally ith th C apping
 at . Th fo th cont ol captu C appo xintly th la C
 . m of th t an ition.

The xi C C mf a iation in h xactly u_2 and y_2 : gin
 and nd du to th C apping at and noi C 2 o f , j_u i
 al ay C allo d to ach , fn if th i C an C that th I C
 ill m dify th f oltag fo di C an C C than . m a y
 f om th catch ing coil

4.2 Selection of desired trajectory

u y t uncating th po tion of th t aj cto y i h to t ac 7,
 haf inadf t ntly int oduc d ano th comp ication. Th
 d C d t aj cto y, y_d , mu t: a C o th xt n C on of y_1
 fo it to : f a C ly t ac 7 d: y y_2 . Sp ci g cally , th po tion
 and f locity at th ta t of y_d mu t h th po tion and
 f locity at th nd of y_1 .

To C C thi C on C aint l t

$$y_d[k][j_y] = y_2[k][1] e^{\frac{v[k][1]}{y_2[k][1]}(j_y-1)TS} \quad (6)$$

h $v[k][1]$ i C h f locity of th a nt u h nth C
 $y_2[k][1]$ i C co d d and TS i C th C apping tim
 V C d n gatif falu i C ho C n fo $v[k][1]$ that ill n C
 that y_d d caying xpon ntially and th u C th t ac 7ing o
 d c a C o hould th impact f locity. Th g x d $v[k][1]$
 falu do C not gua ant a C o th t aj cto y; ut it i C a C
 C oution fo th ca C of z o ai T di tu : anc C id ally,
 C could u C a f locity C o fo an accu at falu of th
 initial f locity o C could u C th C t i n d f locity f om
 th o: C f in ().

4.3 Noise compensation

To p f nt th I C f om t m m ing to comp at fo C C
 noi C th ma C d t aj cto y n d C to : g lt d. S hil
 th o: C f do C g lt th output, it do C not comp ly
 limit th noi C V gain, th p t i f natu of th C t m
 i C xploit d to imo f th g lt ing.

In C ad of uplating f y cycl, th I C i C nd i g d to updat
 f y thi d cycl. Th t ac 7ing o i C h u d t im d: y
 th diff nc : t n th d C d t aj cto y and th af ag
 of th p fiou C th ma C d t aj cto i C Equation (5) i C
 no g if n : y

$$u[n+1] = Su[n] + Ey_{error} \text{ fo } n = 3k \quad (7)$$

$$u[n+1] = u[n] \text{ fo } n \neq 3k \quad (8)$$

h

$$y_{error} = y_d - \frac{1}{3} \sum_{j=0}^2 y[n-j]. \quad (9)$$

5 Experimental results

The follo ing xp imm t C a conduct d to gaug th ff c-
 tif n C of th I C. If ll tun d, th nonlin a f d: ac 7 gif n
 : y equation (2) achi f C impact f lociti C ith a man of
 . 6 m C th output of th ll tun d nonlin a f d: ac 7
 nte h th d C d t aj cto y clo C ly, a C ho n in igu 4.
 Th f C p n C i C al o includ d in igu 4 fo comp ication.

In ach xp imm t th f d: ac 7 i C tu : d igh tly, and th
 I C i C u C d to t ac 7 th d C d t aj cto y. o con C tency
 ith ou p fiou C o 7 4, 5, 7] th po tion plott d in th
 follo ing g gu C i C th d fiation f om th ind l po tion (4
 m l i C an C f om th coil).

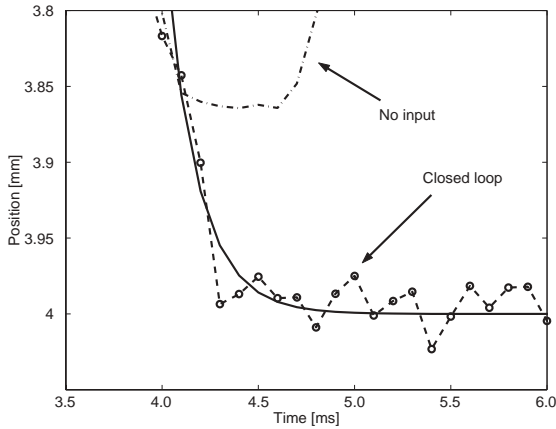


Figure 4 Comparison of the desired trajectory and the output achieved by a well-tuned feedback controller.

5.1 Matched perturbation

One of the experiments that failed during the first run was that the input field collapsed during the period. When the input collapsed, the controller was unable to handle it.

The average of the first 100 of the trajectory and the average of the 10th 100 of the trajectory and the desired trajectory are plotted together for comparison in Figure 5. Initially the trajectory is quite lagged and the amplitude is again the catching coil. In this situation, the output is much lower and the overshoot is significantly larger.

The change in the input voltage during the first and 10th iterations is shown in Figure 6. The dotted line plots the voltage that would have been given by the non-tuned feedback controller.

5.2 Detuned feedback

In this section the feedback is tuned throughout the trajectory, while the input field is fixed to acting on the first and second magnetic coils. The gain of the non-tuned feedback is adjusted such that the non-tuned feedback, V_{fb}^+ , is always greater than the nominal feedback, V_{fb}^- . In Figure 7 and 8 the input field is adjusted in the trajectory to achieve the trajectory of the desired trajectory.

If the gain of the non-tuned feedback is adjusted such that the non-tuned feedback, V_{fb}^- , is always less than the nominal feedback, V_{fb}^+ , then the catching coil will no longer touch the catching coil, and the system will not be initialized to the target position. When the point is set to be initialized to the target position, the system will not be initialized to the target position. When the point is set to be initialized to the target position, the system will not be initialized to the target position.

The comparison of the performance of the feedback controller.

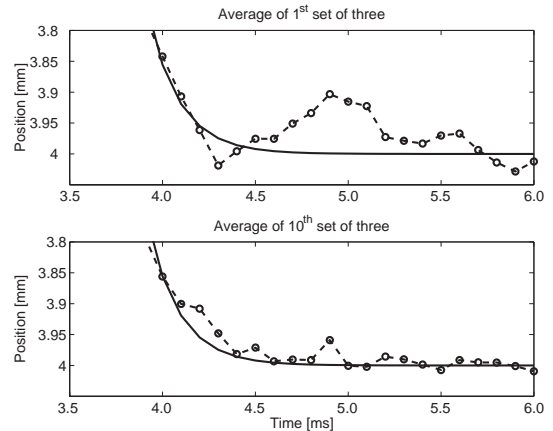


Figure 5 Comparison of the 1st and 10th iteration for the matched perturbation case.

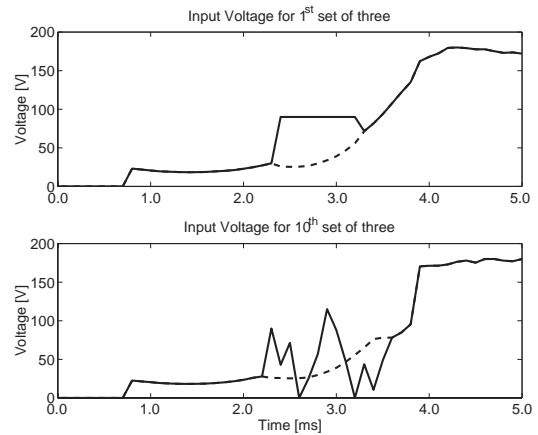


Figure 6 Comparison of the 1st and 10th iteration input voltage for the matched perturbation case.

5.3 Performance deterioration

One of the previous experiments concerned the output and the desired trajectory sufficiently well, the performance degraded. This is shown in Figure 9, and highlights the output, input voltage, and 2-norm of the error.

The dynamics of the system exhibit non-monotonic behavior that causes the initial configuration to follow the desired trajectory. The configuration of the system at different points along the trajectory is different. In our case, a large difference in the landing of the target against the catching coil, which is a result of the initialization procedure. The configuration/difference of individual points along the trajectory are plotted in Figure 10 and 11. From the plot it appears that the error difference at the 10th iteration.

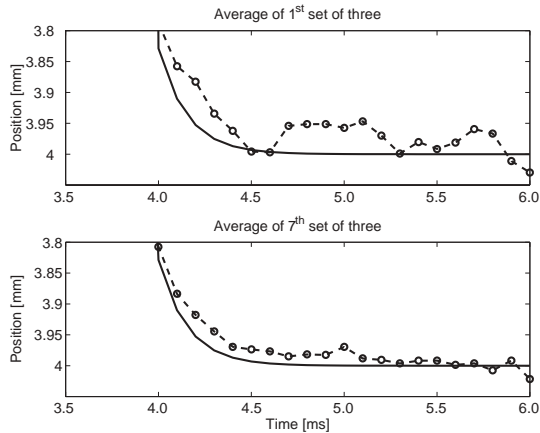


Figure 7 Comparison of the 1st and 7th iteration for V_{fb}^+

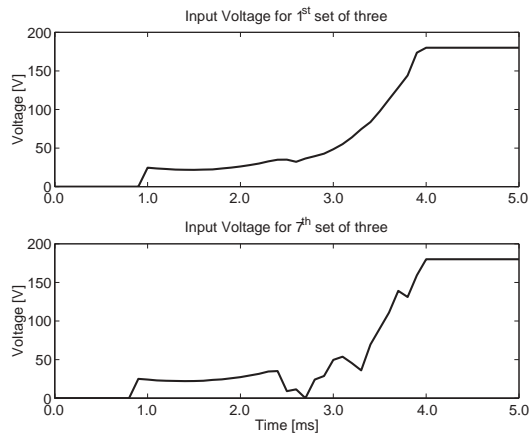


Figure 8 Comparison of the 1st and 7th iteration input voltage for V_{fb}^+

- 1. Point at the beginning of the trajectory a not noticeable convergence.
- 2. Point in the middle of the trajectory convergence slowly.
- 3. Point at the end of the trajectory convergence quickly.

Due to the significant nonlinearities in the system a tracking controller, convergence at a point is not accurate enough to not monotonic behavior at all points in the trajectory.

5.4 Impact velocity

Since tracking error in Section 5.2, it is important that the impact velocity decrease as all V_{fb} plotted in Figure 4, the impact velocity decrease with IC do not achieve impact velocity as a whole as highlighted in [4, 5]. Perhaps if the IC can improve to avoid the performance deterioration in Section 5. The impact velocity

could decrease a further.

6 Conclusion

Since the iterative learning control is applied to improve the tracking performance of the electromechanical valve actuator, it is effective in the following factors:

- 1. Control robustness
- 2. Process gain capability
- 3. Maximum time of IC

The methodology presented here attempts to account for the controller but does not offer compensation completely. Therefore, experimental results do not indicate in the tracking of a 7 millisecond signal that the development of a more accurate convolution matrix to avoid the convergence followed by divergence phenomenon.

Acknowledgements

Support provided by the National Science Foundation under contract S-ECS-49 and the Motorola Company through a 2 University Research Project.

References

- [1] Doh, T.Y., Moon J.H., Jin, K.B., and Chung, M.J., "An iterative learning control for uncertain systems using structured singular value". In Proceedings of the 2nd Asian Control Conference, Seoul Korea, July 1997. 61
- [2] Huang, Y.C., Longman, R.W., "The source of the often observed property of Initial convergence followed by divergence in learning and repetitive control". Advances in astronautical sciences, Vol: 90 pages: 555-572.
- [3] Hoffmann W., Stefanopoulou A., "Iterative Learning Control of Electromechanical Camless Valve Actuator," Proceedings American Control Conference, pp.2860-2866, June 2001.
- [4] Peterson, K., Stefanopoulou A., Haghgoie M., Megli, T. "Output Observer Based Feedback for Soft Landing of Electromechanical Camless Valve Actuator", to be presented at the American Control Conference 2002.
- [5] Peterson, K., Stefanopoulou A., Wang Y., Haghgoie M., Megli, T. "Nonlinear self tuning control for soft landing of an Electromechanical Valve Actuator", To be presented at the IFAC on mechatronics 2002.
- [6] Tai, C., Stubbs, A., Tsao, T.C., "Modeling and Controller Design of Electromagnetic Engine Valve". Proceedings of American Control Conference, pp. 2890-2895, June 2001
- [7] Wang Y., Stefanopoulou A., Peterson K., Megli T., Haghgoie M., "Modeling and Control of Electromechanical Valve Actuator", SAE 2002-01-1106.

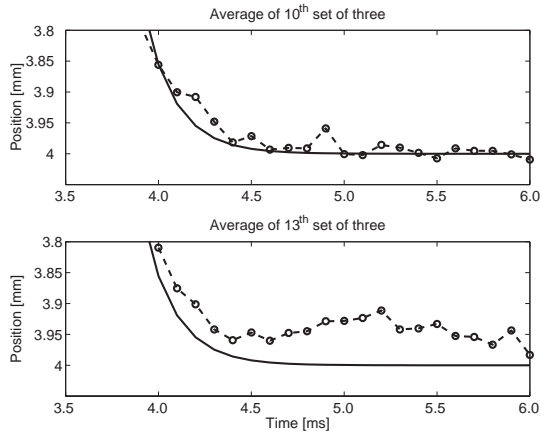


Figure 1 Comparison of the 10th and 13th iteration for the average of three data points

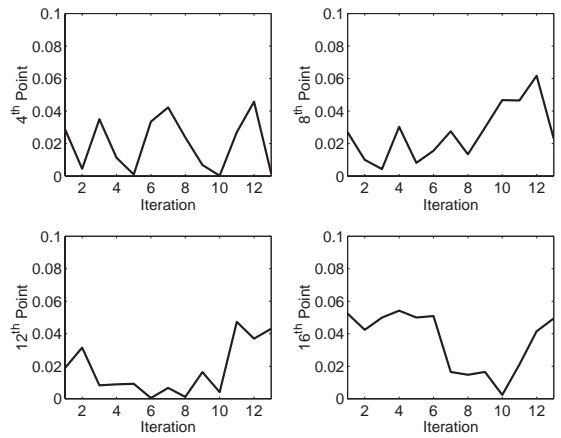


Figure 2 Configuration/Difference of the 4th, 8th, 12th, and 16th points in the trajectory

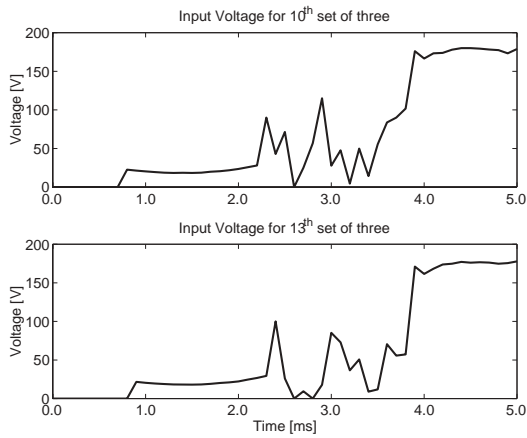


Figure 3 Comparison of the 10th and 13th iteration input voltage for the average of three data points

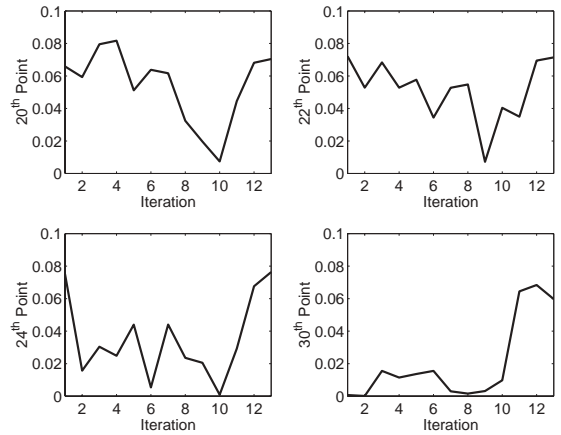


Figure 4 Configuration/Difference of the 20th, 22th, 24th, and 30th points in the trajectory

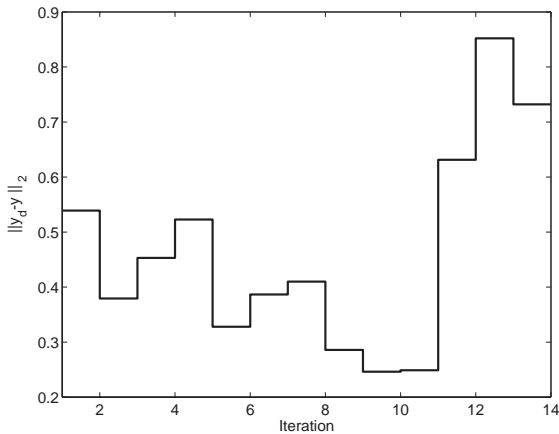


Figure 5 The 2-norm of the derivative of the position

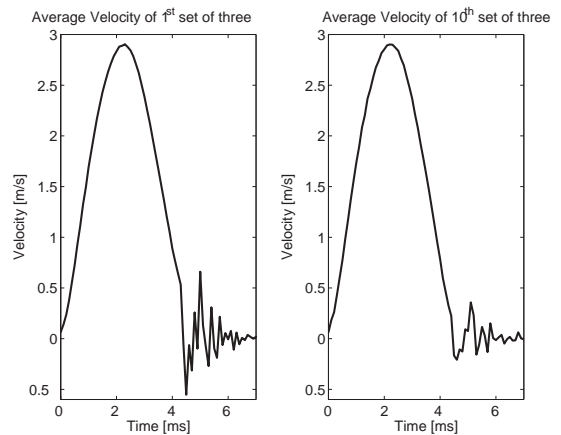


Figure 6 Velocity of the 1st and 10th Iteration